Real-time, in vivo confocal reflectance microscopy of basal cell carcinoma

Salvador González, MD, PhD, and Zeina Tannous, MD *Boston, Massachusetts*

Background: Real-time, near-infrared confocal laser scanning microscopy may provide a way to diagnose basal cell carcinoma in vivo and might potentially eliminate the need for invasive diagnostic biopsies in the future.

Objective: The purpose of this study is to define the in vivo histologic features of basal cell carcinoma by using a high-resolution imaging technique.

Methods: Five fair-skinned white patients with 8 basal cell carcinoma lesions were recruited for this study. Near-infrared reflectance confocal microscopy imaging was used to characterize the histologic features of these lesions in vivo. Subsequently, the confocal histologic features were correlated with the corresponding routine hematoxylin-and-eosin-stained sections obtained from invasive biopsies.

Results: A uniform population of basal cell carcinoma cells with characteristic elongated nuclei oriented along the same axis was always present. Abundant blood vessels demonstrating prominent tortuosity were seen, as well as prominent, predominantly mononuclear inflammatory infiltrate admixed or in close apposition with basal cell carcinoma cells. Trafficking of leukocytes was visualized in real time.

Conclusion: Our results demonstrate that near-infrared confocal microscopy may facilitate diagnosis of basal cell carcinoma with the use of in vivo high-resolution confocal features. Accuracy studies to evaluate these in vivo histologic criteria are warranted. (J Am Acad Dermatol 2002;47:869-74.)

I n 1995, we reported the construction of a near-infrared confocal scanning laser microscope for imaging human skin in vivo.[1] Like standard confocal microscopes, this microscope has the capability to optically section turbid objects with good contrast and resolution without the need for tissue fixation and processing before visualization.[2-4] When this technique is used, a low-power laser beam is focused tightly on a specific point in the tissue, detecting only the light that is back-scattered from the plane in focus, with contrast caused by native variations in the refractive index of tissue microstructures. Advances in confocal microscopy with optimization of optical parameters such as use of near-infrared lasers as the light source, immersion media matching, and objective lenses with higher numeric aperture (NA) have provided greater resolution and contrast to a depth of 300 to 350 μm, as well as better access to different topographic areas.[5,6]

Our group has recently reported that confocal microscopy may facilitate the in vivo viewing of the microscopic features of several inflammatory skin conditions such as psoriasis,[7] allergic contact dermatitis,[8] sebaceous gland hyperplasia,[9,10] and actinic keratoses.[11]

The aim of our study is to define the in vivo histologic features of basal cell carcinoma (BCC) by using noninvasive, real-time confocal microscopy. Our results demonstrate that confocal microscopy may facilitate diagnosis of BCC with the use of in vivo high-resolution confocal features.

METHODS
Subjects

Five fair-skinned patients with 8 skin lesions located on the face, forehead, forearms, legs, and abdomen were recruited for our study after signed informed consent documents were obtained under a Massachusetts General Hospital Institutional Review Board-approved protocol. The group included 3 men and 2 women with ages ranging from 42 to 81
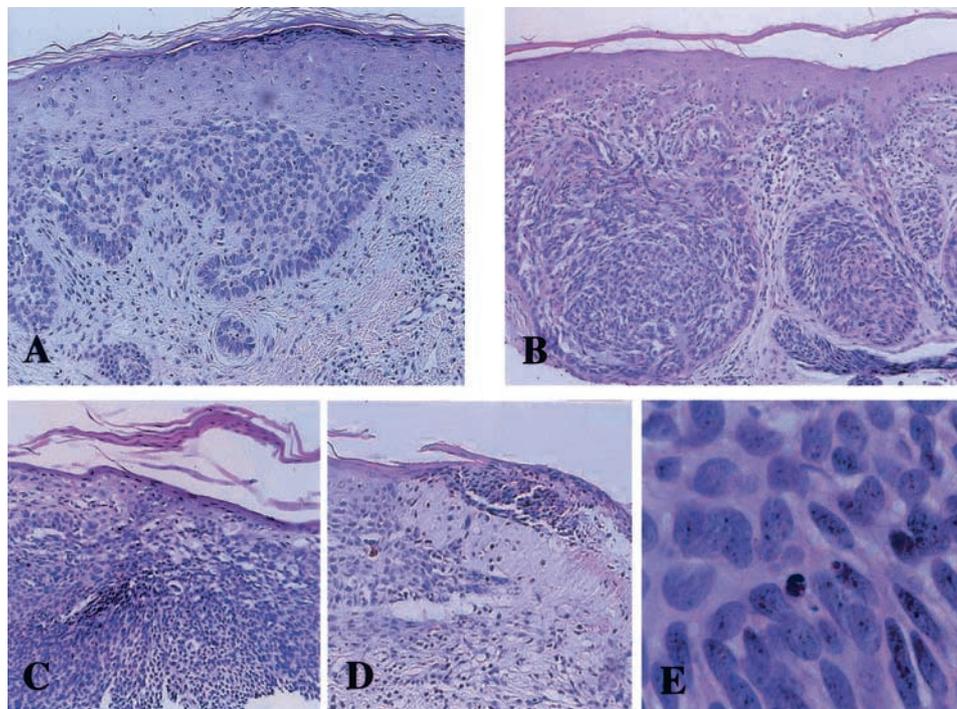
Fig 1. A, Basal cell carcinoma (BCC) of superficial type. **B,** BCC of nodular type. **C,** Parakeratosis and keratinocytic atypia overlying BCC. **D,** Parakeratosis and a subcorneal pustule overlying superficial BCC with clefting of BCC from surrounding stroma, increased vascularity, and mononuclear inflammatory cell infiltrate in superficial dermis. **E,** BCC cells with hyperchromatic oval to round nuclei and scant, poorly defined cytoplasm.

Table I. Topographic locations and histologic types of lesions

Specimen No.	Site	BCC subtype
1	Forehead	Superficial
2	Right forearm	Superficial
3	Left forearm	Superficial
4	Forehead	Nodular
5	Nose	Superficial
6	Left leg	Superficial
7	Right leg	Superficial
8	Abdomen	Superficial

BCC, Basal cell carcinoma.

years. Five of 8 lesions were recurrent biopsy-proven BCCs (lesions 1-5, Table I), and 3 lesions were clinically consistent with BCC.

Confocal microscopy was performed on 5 lesions after the biopsy was performed (lesions 1-5, Table I) and on 3 lesions before the biopsy procedure (lesions 6-8, Table I). Histopathologic examination of the 8 biopsy specimens revealed features diagnostic of superficial BCC in 7 of 8 lesions and of nodular BCC in 1 of 8 lesions.

Confocal imaging

We used a near-infrared confocal microscope (CM) with illumination at a wavelength of 1064 nm with a neodymium:yttrium-aluminum-garnet laser (CV-4; Santa Fe laser Co, Tucson, Ariz). A detailed description of the system has been recently published.[3,7] Illumination was achieved with a power lower than 40 mW. We used the following water-immersion objective lenses: 30×, 0.9 NA (No. 96008 LOMO; Vermont Optics, Charlotte, Vermont), 60×, 0.85 NA (No. 1UM571, Olympus America Inc, Melville, NY), and 100×, 1.2 NA (No. 518039, Leica, Microsystems Inc, Exton, Pa). Immersion media were sucrose-water solutions at concentrations required for refractive index of 1.34 when imaged with a 100× objective lens, and water or water-based gels (refraction index 1.33) (eg, gels used for ultrasound imaging [Aquasonic 100 gel, Fairfield, NJ] or hair care) for the remaining objective lenses. We found that we obtain the best resolution and contrast when the immersion medium has refractive indices of 1.33 to 1.35. The measured lateral resolution is 0.5 to 1 μm, and the axial resolution (section thickness) is 3 to 5 μm to a controlled depth of 200 to 350 μm in healthy human skin.[5]

The imaging is at video rates, and hence the

Table II. Histologic features seen with routine staining and in vivo confocal imaging

Histologic features	H&E-stained sections	In vivo confocal imaging
Parakeratosis	+	+
Actinic changes	+	+
Monomorphism of cells	+	+
High N/C ratio	+	+
Elongated nuclei	+	+
Prominent nucleoli	+	+
Increased vascularity	+	+
Inflammatory cells	+	+
BCC subtypes	+	+
Polarization of nuclei	−	+
Rolling of WBCs	−	+
Mucin	+	+/−
Solar elastosis	+	+/−
Amyloid	+	−
Clefting	+	−
Palisading	+	−

BCC, Basal cell carcinoma; *H&E*, hematoxylin and eosin; *N/C*, nucleo-cytoplasmic; *WBCs*, white blood cells.

Fig 2. Confocal image of an impetiginized basal cell carcinoma in vivo. Parakeratosis (ie, nuclear retention [*arrows*] in horny layer [SC] is seen along with subcorneal pustule of polymorphonuclear neutrophils [*arrowheads*]). (Hematoxylin-eosin stain, original magnification ×100; 1.2 numeric aperture (NA) water-immersion objective lens. Scale bar, 25 μm.)

images were observed in real time on a TV monitor (Sony Trinitron, Tokyo, Japan). We either video-taped the images with a superVHS videotape recorder (Panasonic AG 7300, Panasonic Consumer Electronic, Secaucus, NJ) or captured them with an 8 bits/pixel frame grabber (model Pixelpipeline PTP425; Perceptics, Knoxville, Tenn). Details are reported elsewhere.[5]

Data analysis

Features analyzed by confocal microscopy included morphologic characteristics such as nuclear shape, cytoplasmic appearance, tumor pattern, epithelial cell-to-epithelial cell interaction, cell density, characteristics of the inflammatory infiltrate, morphology of the dermal microvasculature, and gross appearance of the connective dermal tissue.

Hematoxylin-and-eosin (H&E)-stained histologic vertical sections of these 8 lesions were correlated with the corresponding en face horizontal confocal images.

RESULTS
Histopathologic features

Eight biopsy specimens from 5 patients were examined. All these specimens exhibited characteristic histopathologic features of BCC with two morphologic subtypes, superficial (7 specimens, Fig 1, *A*) and nodular (1 specimen, Fig 1, *B*). The histologic features on formalin-fixed, paraffin-embedded tissues included parakeratosis; actinic changes in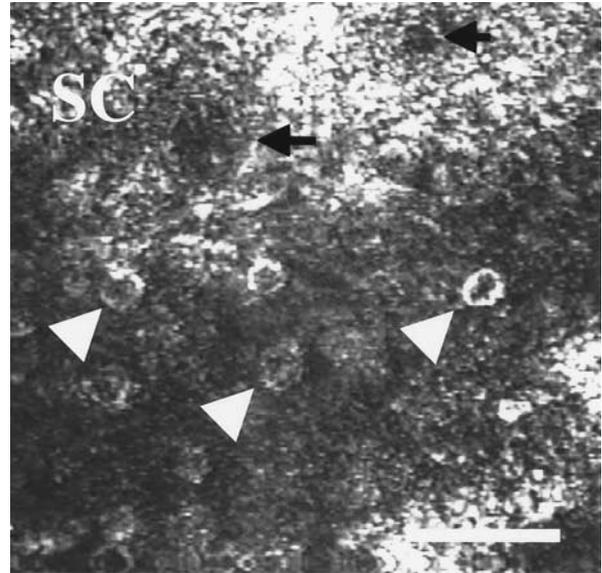 the overlying epidermis, islands of basaloid cells with monomorphic hyperchromatic nuclei, and scant poorly demarcated cytoplasm; mitotic figures; apoptotic cells; and palisading of the basaloid cells at the periphery of the islands (Table II, Fig 1, *A-E*). These islands of tumor cells were surrounded by an abundant mucinous stroma with separation of the tumor cells from the surrounding stroma (clefting). Prominent increased vascularity was also noted, as well as solar elastosis and variable amounts of predominantly mononuclear inflammatory cells with scattered neutrophils. One biopsy specimen revealed a subcorneal collection of neutrophils (Fig 1, *D*, and Fig 2). Another biopsy specimen (specimen No. 2) demonstrated amyloid deposition within the tumor islands.

Confocal features

At low-power magnification (Table II), islands of tumor cells were noted with high refractility, associated with intervening areas of low refractility, which might correspond to the mucinous stroma. Abundant blood vessels were seen juxtaposed to BCC cells with rolling of leukocytes along the endothelial lining (Fig 3, *A-D*). Also intermixed with the BCC cells were inflammatory cells, mainly mononuclear cells (lymphocytes, Fig 4) with scattered cells with multisegmented nuclei (neutrophils). The overlying epidermis showed some degree of keratinocytic atypia with variably sized nuclei at the basal cell
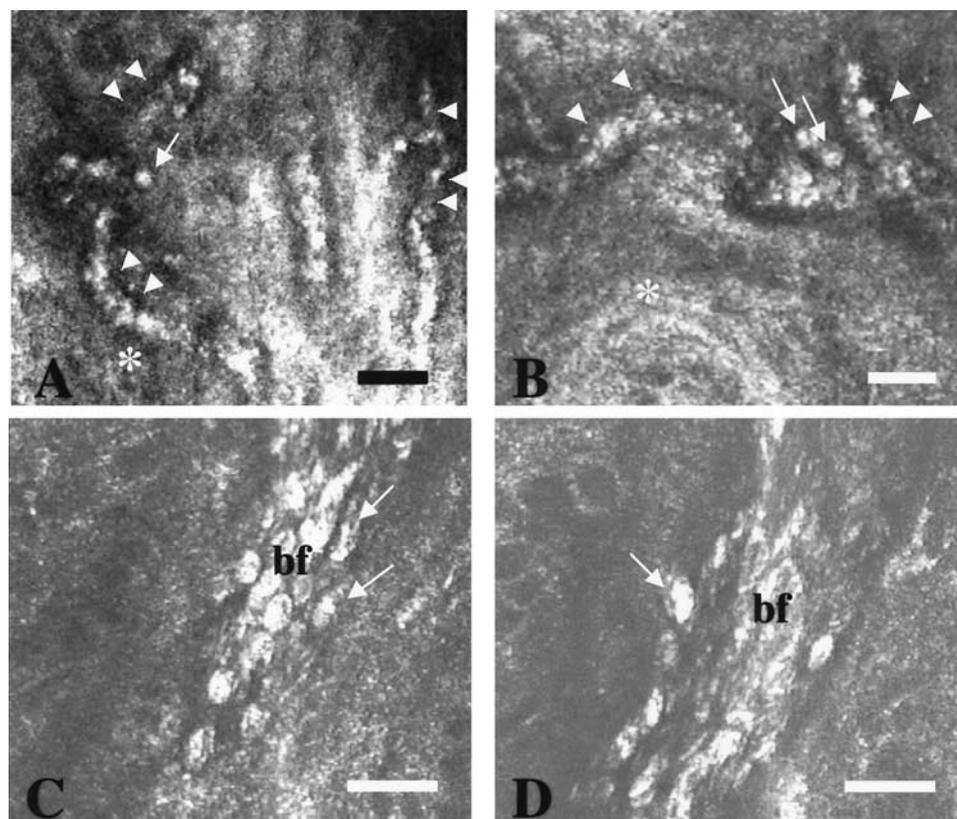
Fig 3. Confocal images showing increased vascularity and tortuosity (*arrowheads*, **A, B**) associated with a basal cell carcinoma, superficial type *(asterisk)*. Inflammatory cells are easily identified as bright, highly refractile round cells along the endothelial lining (*arrows*, **A-D**). Adhesion of individual leukocytes (*arrows*, **A-D**) to endothelial walls is also visualized in real time. Dynamic events mediating leukocyte emigration from vascular compartment to skin can be seen during real-time imaging. Note that blood flow (*bf*) is better seen on real-time video than on still, grabbed images **(C, D)**. (**A-D,** Hematoxylin-eosin stain; original magnifications: **A** and **B,** ×60, 0.85 numerical aperture (NA) water-immersion objective lens; **C** and **D,** ×100, 1.2 NA water-immersion objective lens. Scale bar, 25 μm).

layer, pleomorphism, architectural disarray, and parakeratotic nuclei in the stratum corneum (Fig 2).

The BCC cells appeared to be elongated with their nuclei oriented along the same principal axis, thus manifesting a polarized appearance (Fig 5, *A*). These tumor cells had a high refractive index with dark appearing nuclei (low contrast), whereas the cytoplasm appeared bright. They were monomorphic in shape with a high nucleocytoplasmic ratio and sometimes contained prominent nucleoli, which appeared bright in color (Fig 5, *B* and *C*; Fig 1, *E*). Nesting and nodularity of epithelial cells at the papillary dermal level were easily identified in the only lesion with a biopsy-proven nodular BCC (lesion 4, Table I). Solar elastosis was detected with relative uncertainty in the dermis surrounding the tumor cells. Clefting, palisading, and amyloid deposition were not demonstrated with certainty by confocal imaging.
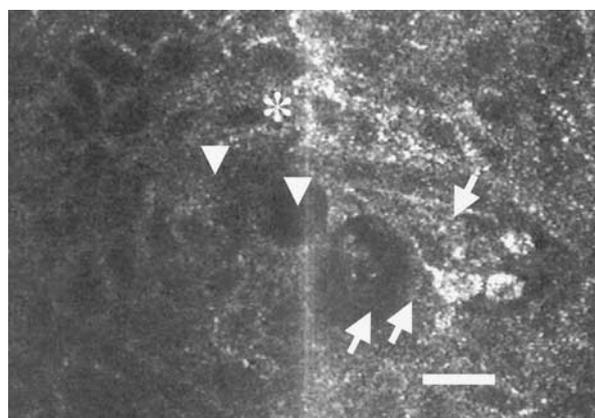

Fig 4. Confocal image of a basal cell carcinoma superficial type in vivo (*asterisk*) showing adjacent and primarily mononuclear perivascular inflammatory infiltrate (*arrows*). (Hematoxylin-eosin stain; original magnification ×100; 1.2 numeric aperture water-immersion objective lens. Scale bar, 25 μm.)
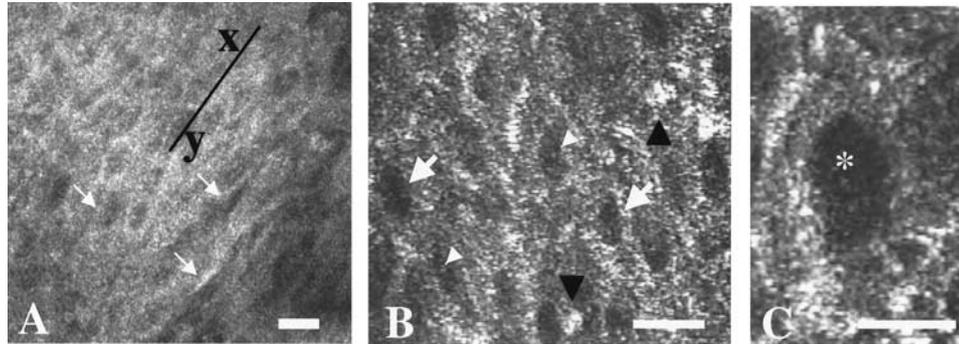
Fig 5. Real-time in vivo confocal images of a basal cell carcinoma (BCC) showing a uniform population of elongated cells (*arrows*, **A** and **B**) oriented along the same principal axis (x-y). Mononuclear cells (*black arrowheads*, **B**) are seen intermixed with BCC cells (*arrows*, **B**) with some of the BCC cells showing nucleoli (*white arrowheads*, **B**). **C,** High-power magnification of one BCC cell demonstrating a large elongated nucleus with a low refractility (*asterisk*), surrounded by a bright cytoplasm. (**A-C,** Hematoxylin-eosin stain; original magnifications: **A,** ×30, 0.9 numerical aperture (NA) water-immersion objective lens; **B** and **C,** ×100, 1.2 NA water-immersion objective lens. Scale bar, 25 μm.)

DISCUSSION

Near-infrared confocal microscopy has proven to be a promising, noninvasive, high-resolution imaging tool for histologic evaluation of the skin in vivo. Recently, the major microscopic features of several premalignant and malignant skin lesions have been reported.[9,12,13] The aim of our study was to define the in vivo confocal features of BCC by using noninvasive, real-time confocal microscopy. We have evaluated the in vivo confocal features of 8 biopsy-proven BCCs (7 superficial BCCs and 1 nodular BCC) in 5 patients. We were able to define specific confocal histologic features that might prove to be useful in the diagnosis of BCC by using real-time confocal microscopy without the need for an invasive biopsy and the time-consuming histologic preparation of the biopsy specimen. We have found that the confocal features correlated very well with the H&E-stained sections of the biopsy specimens. Features that were readily identified by both in vivo confocal microscopy and standard microscopy of H&E-stained sections included parakeratosis, actinic changes overlying the BCC, relative monomorphism of BCC cells, BCC nuclei exhibiting characteristic elongated or oval appearance, high nucleocytoplasmic ratios, and the presence of prominent nucleoli, increased vascularity, and prominent predominantly mononuclear inflammatory cell infiltrate. Features that were detected by in vivo confocal microscopy but not with standard microscopy of H&E-stained sections included uniform polarization of BCC nuclei and rolling of white blood cells along the walls of dermal blood vessels.[14] Features that were detected readily by standard microscopy of H&E-stained sections but were detected with relative un-certainty by in vivo confocal microscopy included mucin deposition and solar elastosis. Features that were detected readily by standard microscopy of H&E-stained sections but were not detected by in vivo confocal microscopy included clefting and palisading of BCC cells and amyloid deposition by tumor cells. Our results demonstrated an excellent correlation between in vivo confocal imaging and standard microscopy of H&E-stained sections. Confocal microscopy may facilitate the in vivo diagnosis of BCC with the use of high-resolution confocal criteria and thus might eliminate the need for the invasive biopsy procedure. Additional studies to test the sensitivity and specificity of in vivo confocal microscopy for diagnosing BCC based on these criteria are in progress.

REFERENCES

1. Rajadhyaksha M, Grossman M, Esterowitz D, Webb RH, Anderson RR. In vivo confocal scanning laser microscopy of human skin: melanin provides a good contrast. J Invest Dermatol 1995; 104:946-52.
2. Wilson T. Confocal microscopy. San Diego: Academic Press; 1990.
3. Pawley JB. Handbook of biological confocal microscopy. 2nd ed. New York: Plenum Press; 1995.
4. Webb RH. Confocal optical microscopy. Rep Prog Phys 1996;59: 427-71.
5. Rajadhyaksha M, Gonzalez S, Zavislan J, Anderson RR, Webb RH. In vivo confocal scanning laser microscopy of human skin II: advances in instrumentation and comparison to histology. J Invest Dermatol 1999;113:293-303.
6. Huzaira M, Rius F, Rajadhyaksha M, Anderson RR, González S. Topographic variations in normal skin histology, as viewed by in vivo confocal microscopy. J Invest Dermatol 2001;116:846-52.

7. Gonzalez S, Gonzalez E, White WM, Rajadhyaksha M, Anderson RR. Allergic contact dermatitis. Correlation of in vivo confocal imaging to routine histology. J Am Acad Dermatol 1999;40:708-13.

8. Gonzalez S, Rajadhyaksha M, Rubinstein G, Anderson RR. Characterization of psoriasis in vivo by reflectance confocal microscopy. J Med 1999;30:337-56.

9. Aghassi D, Anderson RR, Gonzalez S. Confocal laser microscopic imaging of actinic keratoses in vivo: a preliminary report. J Am Acad Dermatol 2000;43:42-8.

10. González S, White WM, Rajadhyaksha M, Anderson RR, González E. Confocal imaging of sebaceous gland hyperplasia in vivo to assess efficacy and mechanism of pulsed dye laser treatment. Lasers Surg Med 1999;25:8-12.

11. Aghassi D, Anderson RR, González S. Time-sequence histologic imaging of laser-treated cherry angiomas using in vivo confocal microscopy. J Am Acad Dermatol 2000;43:37-41.

12. Langley RGB, Rajadhyaksha M, Dwyer PJ, Sober AJ, Flotte TJ, Anderson RR. Confocal scanning laser microscopy of benign and malignant melanocytic lesions in vivo. J Am Acad Dermatol 2001;45:365-76.

13. Bussam KJ, Hester K, Charles C, Sachs DL, Antonescu C, González S, et al. Detection of clinically amelanotic malignant melanoma and assessment of its margins by in vivo confocal scanning laser microscopy. Arch Dermatol 2001;137:923-9.

14. González S, Sackstein R, Anderson RR, Rajadhyaksha M. Real-time evidence of in vivo leukocyte trafficking in human skin by reflectance confocal microscopy. J Invest Dermatol 2001;117:384-6.